C-RED One and C-RED 2: SWIR advanced cameras using Saphira e-APD and Snake InGaAs detectors

,Philippe Feautrier[a,b,*], Jean-Luc Gach[a,c], Timothée Greffe[*a] , Fabien Clop[a], Stephane Lemarchand[a], Thomas Carmignani[a], Eric Stadler[a,b],Carine Doucouré[a] and David Boutolleau[a]

[a]First Light Imaging S.A.S. 100, Route des houillères, 13590 Meyreuil, France;
[b] Univ. Grenoble Alpes, CNRS, IPAG, F-38000 Grenoble, France ;
[c]Aix Marseille Université, CNRS, LAM (Laboratoire d'Astrophysique de Marseille) UMR 7326, 13388 Marseille, France;

*philippe.feautrier@first-light.fr; phone +33 6 31 08 26 95, www.firstlight.fr

ABSTRACT

After the development of the OCAM2 EMCCD fast visible camera [1] dedicated to advanced adaptive optics wavefront sensing, First Light Imaging moved to the SWIR fast cameras with the C-RED One and the C-RED 2 cameras. These cameras and their performances are described extensively in this paper.

First Light Imaging C-RED One infrared camera is capable of capturing up to 3500 full frames per second with subelectron readout noise and very low background. C-RED One is based on the last version of the SAPHIRA detector developed by Leonardo UK. This breakthrough has been made possible thanks to the use of an e-APD infrared focal plane array which is a real disruptive technology in imagery. C-RED One is an autonomous system with an integrated cooling system and a vacuum regeneration system. It operates its sensor with a wide variety of read out techniques and processes video on-board thanks to a Xlinks embedded FPGA.

In addition to this project, First Light Imaging developed an InGaAs 640x512 fast camera with unprecedented performances in terms of noise, dark and readout speed for equivalent products. This camera is based on the SNAKE SWIR detector from Sofradir and was called C-RED 2. The C-RED 2 characteristics and performances are also fully described in this paper.

The C-RED One project has received funding from the European Union's Horizon 2020 research and innovation program under grant agreement N° 673944. C-RED2 development is supported by the "Investments for the future" program and the Provence Alpes Côte d'Azur Region, in the frame of the CPER.

Keywords: infrared camera, e-APD, MCT, high speed, low noise, InGaAs, SWIR, 640 x 512 InGaAs.

1. INTRODUCTION

The Saphira Detector

Designed and fabricated by Leonardo UK, formerly Selex, the Saphira detector is designed for high speed infrared applications and is the result of a development programme alongside the European Southern Observatory on sensors for astronomical instruments [2], [3], [4]. It delivers world leading photon sensitivity of <1 photon RMS with Fowler sampling and high speed non-destructive readout (>10K frame/s). Saphira is an HgCdTe avalanche photodiode (APD) array incorporating a full custom ROIC for applications in the 1 to 2.5µm range.

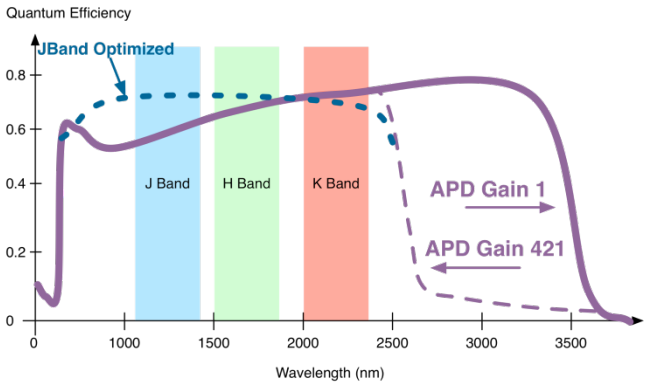

Fig. 1: The SELEX SAPHIRA Mark13 Quantum Efficiency.

The SAPHIRA detector uses the HgCdTe APD properties, offering sub-electron noise with multiplication gain up to x400. The pixel format is 320x256 pixels with 15fF integration node capacitance (28fF with HgCdTe diode). The array has 32 parallel video outputs, organized as 32 sequential pixels in row. The 32 outputs are arranged in such a way that the full multiplex advantage is available also for small sub-windows. Non-destructive readout schemes with subpixel sampling are possible. This reduces the readout noise at high APD gain well below the sub-electron level at frame rates exceeding 1 KHz. The growth technology used now is the metal organic vapour phase epitaxy (MOVPE). This growth technology provides more flexibility for the design of diode structures. It is possible to make heterojunctions with different bandgap properties between the absorption region and the multiplication region. The change to MOVPE resulted in a dramatic improvement in the cosmetic quality with 99.97 % operable pixels at an operating temperature of 85K. The avalanche gain is controlled by an external voltage. The digital and analog functions are controlled by a serial interface. The readout of Saphira allows to read multiple windows, each independently resettable. Glow protection and APD protection circuit are also included.

The Fig. 2 shows the functional bloc diagram of the ME1000 SAPHIRA readout circuit used currently in C-RED. The ME1000 scanning modes include a Read-Reset-Read per row function, so the user can have complete control of the correlated-double-sampling process. Saphira ME1000 incorporates also glow suppression by using 100% metal screening. A reset current limit function has been added in this readout circuit version to protect the array from short circuit APDs.

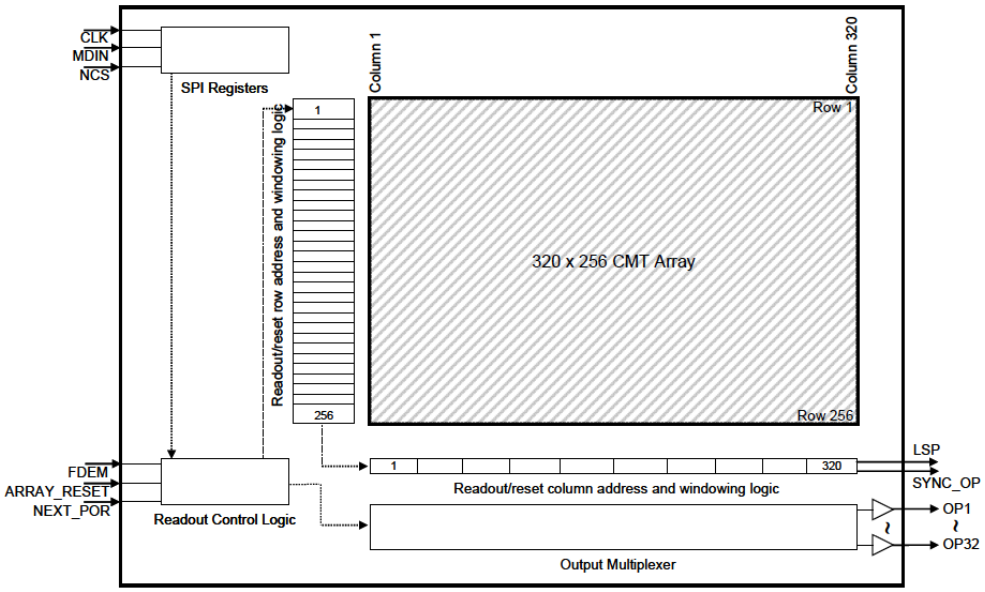

Fig. 2: the SELEX SAPHIRA ME 911/ ME1000 readout circuit architecture.

The C-RED One camera characteristics and performances

The C-RED one camera has the following main characteristics:

- MCT near IR Avalanche Photo Diode 320X256 with Selex Saphira detector.
- Sub-electron readout noise,
- 32 outputs, up to 3500 fps in single read mode.
- Mean Readout noise at 3500 fps and gain 60 <1 e^-.
- 70% QE.
- Supported readout modes: read-reset-read per row, non destructive readout, rolling reset, CDS with read-reset-read per row, multiple line/pixel read
- Pulse tube packaging cooling down to 70 K
- Custom design available (beam aperture)
- Cameralink full data interface

The C-RED One Architecture

C-RED One is an autonomous plug-and-play system with a user-friendly interface, which can be operated in extreme and remote locations.

The sensor is placed in a sealed vacuum environment and cooled down to cryogenic temperature using an integrated pulse tube. The vacuum is self-managed by the camera and no human intervention is required.

The controller is divided in different functional parts as shown in the following block diagram (see Fig. 3).

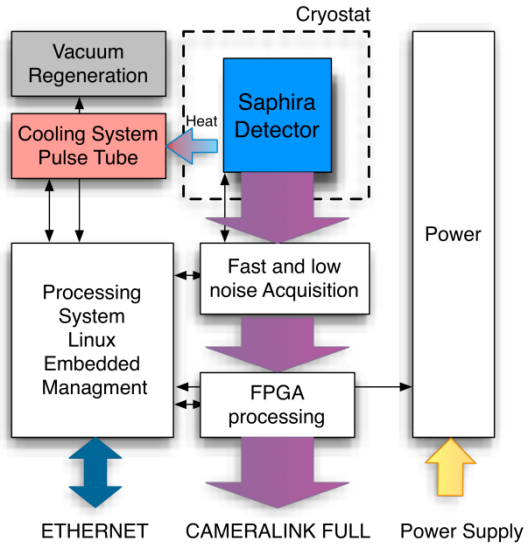

Fig. 3: Architecture of C-RED One.

A Power Board supplies all the subsystems of the camera and is in charge of the cooling systems. It monitors the global current consumption and cut the power if a given threshold is exceed. It also protects the camera against a wrong polarity of the supply.

A Frontend Board supplies and drives the sensor with correct signals and DC bias. A self-monitoring of every voltage is done to avoid any wrong polarization which could damage the sensor. The Frontend Board also digitizes the 32 analogic video signals of the e-APD matrix thanks to a fast and low noise amplification chain.

The Motherboard host a System-On-Chip with two ARM processors and a FPGA. They are both linked with an internal High Speed Bus. The two ARM processors run an embedded Linux and manage every subsystems of the camera. They can also provide video stream to the CameraLink interface or acquire one from the sensor. The FPGA handles the raw data flow coming from the frontend board and processes it to deliver an intelligible video in accordance to the CameraLink standard.

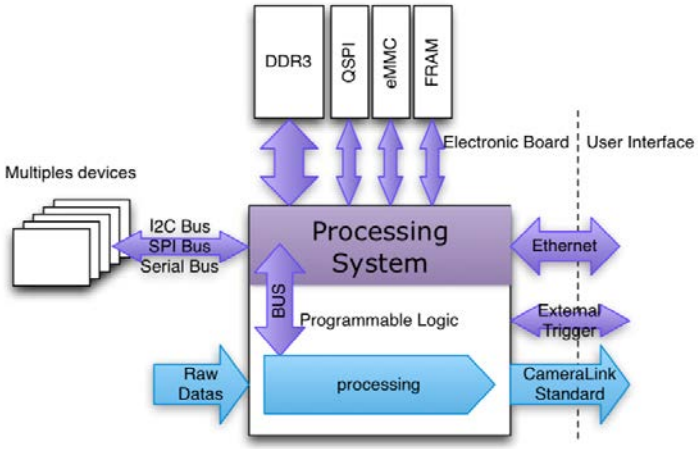

Fig. 4: Architecture of the MotherBoard and System-On-Chip.

The electronic interface is smart and limited to a Power connector, 2 mini CameraLink connectors, one Ethernet port and eventually four Lemo connectors if external triggering and synchronization is needed.

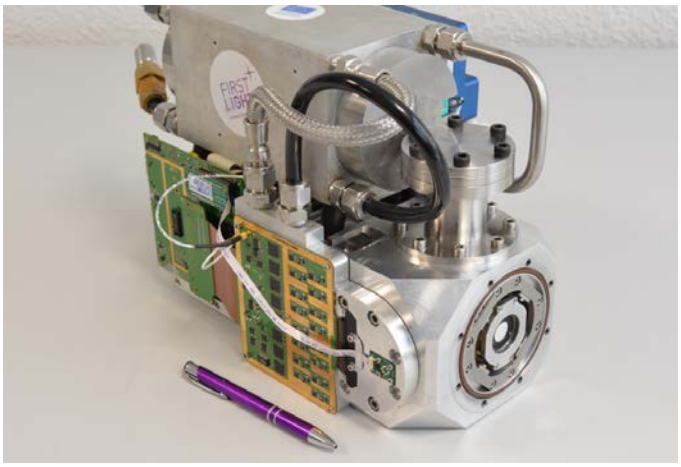

Fig. 5: C-RED One prototype without it outer skin. The pulse tube compressor can be seen on the top whereas in the bottom are the vacuum cryostat and the readout electronics. The purple pen gives the scale..

2. MEASURED C-RED ONE PERFORMANCES

The measurements were all made at 80K operating temperature, using a MARK 13 engineering grade SAPHIRA device.

Quantum efficiency

The array quantum efficiency peaks up to near 80% and the array AR coating may be optimized on a per-device basis for J, H or K bands. Fig. 6 shows the effect of this QE optimization. Moreover due to junction heterostructure with 3.5µm cutoff wavelength HgCdTe material for the avalanche multiplication region and 2.5 µm material for the absorber, the device is sensitive in L band at gain 1 but not with APD gain. This is due to photon penetration depth (longer wavelength photons penetrate deeper in the material and therefore are less amplified). We've measured that already with low gains (in the range of 5 to 10) the L band sensitivity is decreased to near zero, leaving only J, H and K sensitivity.

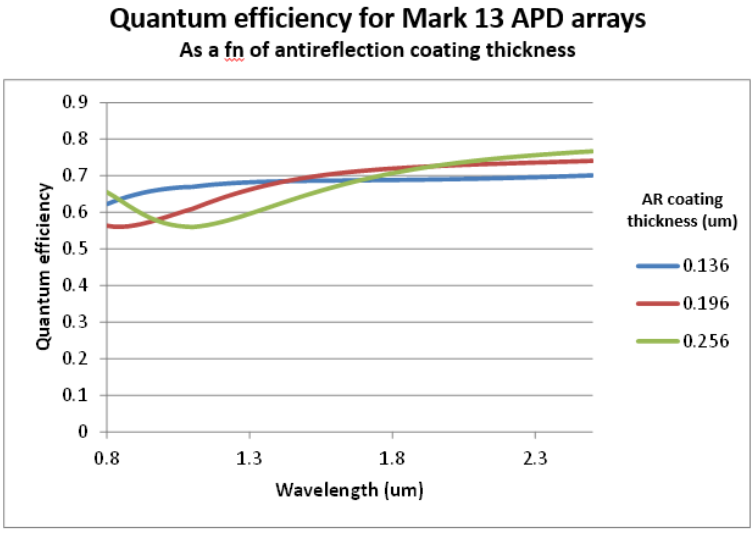

Fig. 6: AR coating and QE optimization for J, H or K bands of Mark13 e-APD diodes.

System gain

The system gain is measured illuminating the sensor with a flat field through an integrating sphere. Then temporal noise versus illumination level is plotted in log/log scale to have the system gain and the noise level (see Fig. 7). The system gain in an infrared device depends strongly upon the diode polarization. Indeed the diode capacitance is used to integrate the charges and its value depends on the reverse voltage applied (the higher, the lower is the diode capacitance). For a 2V reverse bias, which corresponds to a gain of 1, the system gain was measured at 1.1e^-/ADU which is in perfect accordance with the expected 1.15 e^-/ADU system gain with a 28fF node capacitance.

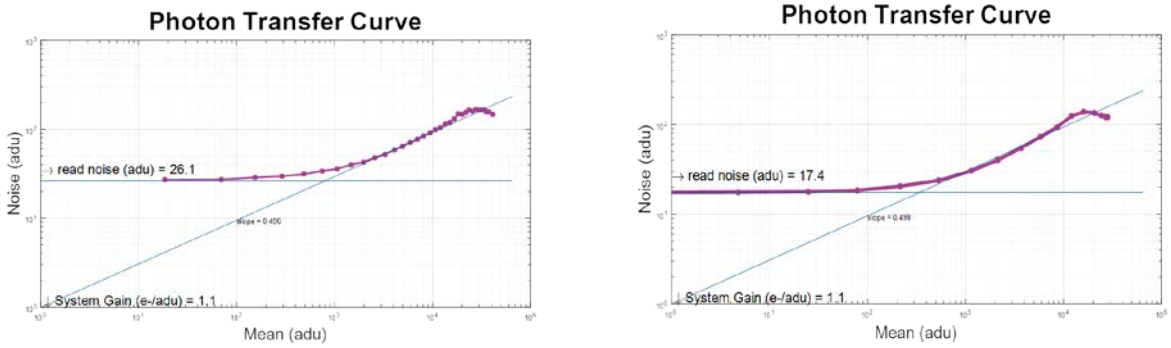

Fig. 7: Photon transfer curve of single readout mode (left) and CDS mode (right).

APD gain

APD gain is measured by illuminating the sensor with a weak laser light at 1300nm. APD gain is then applied, and the ratio of ADU change over reference level gives the gain. To get rid from any FPN (Fix Pattern Noise), the level measurement is done computing the electron flow in multiple non-destructive mode. Fig. 8 shows that APD gain vs bias voltage and the exponential fit. The gain can be expressed as $G=0.309e^{0.395Vbias}$ which is in accordance with other measurements carried out by various groups using these devices.

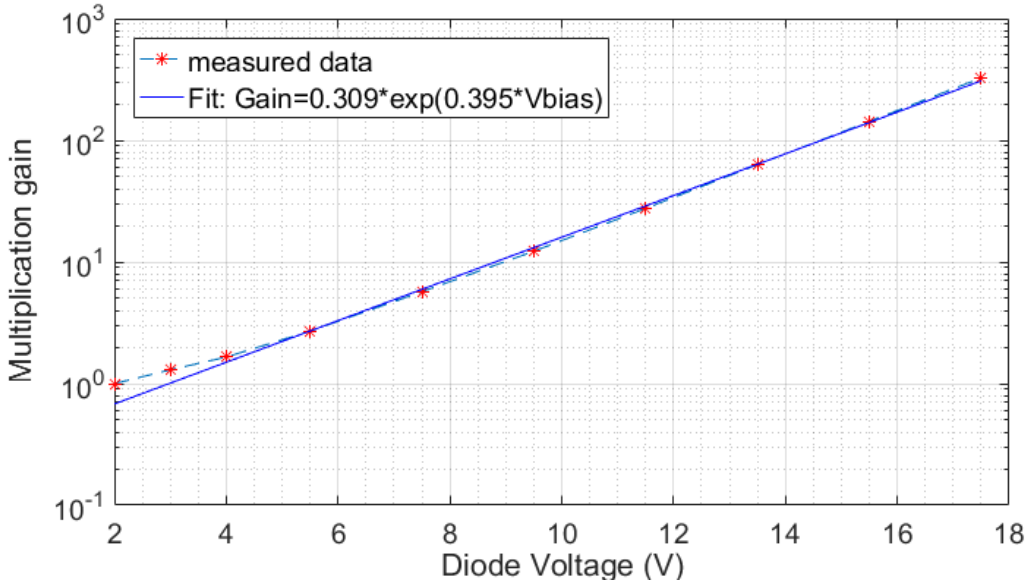

Fig. 8: Measured APD gain vs polarization voltage of MARK 13 array and exponential fit.

System noise

The noise measurement is done by measuring the temporal variation of the image, sensor in the dark looking at a Room temperature blackbody. Measurements have been done for single readout and multiple non-destructive readouts on x-axis and for gain from 1 to 300 on y-axis.

Taking into account 28fF node capacitance, the KTC noise should be in the range of 35e- at 80K. Fig. 9 shows the sensor readout noise as a function of the readout speed and multiplication gain. The readout speed variation is obtained by using either single read mode of multiple non destructive readout. It can be noticed also that for gains > 30, the array enters in subelectron readout whatever is the readout mode (single readout or CDS). This is really a change of paradigm in the way of operating infrared arrays since CDS is no more needed to minimize readout noise, simply by increasing the APD gain, one can have very low noise operation, without compromise on readout speed, but at the expanse of a lower dynamic range.

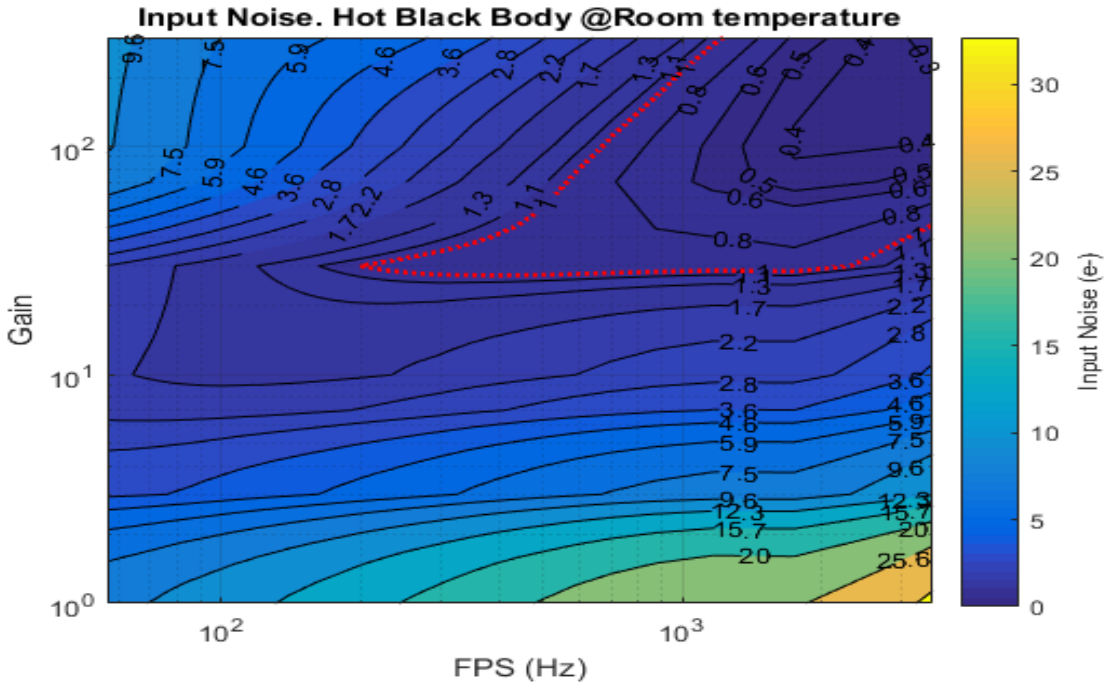

Fig. 9: Measured input referred readout noise of C-RED One vs APD gain for single readout and CDS readout.

Dark current

To do this measurement the sensor is in the dark, looking at a 80K blackbody. The dark current is measured by fitting a line over the ADU level vs exposure time graph. The slope of this line gives the mean dark count in ADU/s.

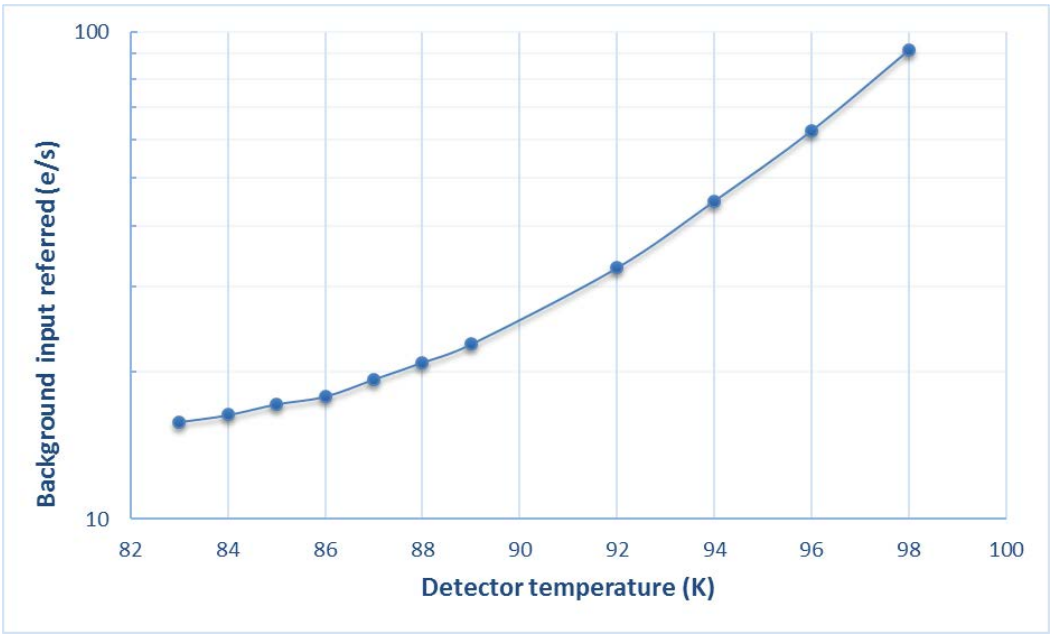

Fig. 10: Measured dark current vs temperature.

Background measurement

The background current is measured the same way it is for the dark current but looking at a room temperature blackbody with a F/4 beam aperture.

The operation is repeated for several gains. The result is plotted in Fig. 11. The evidence is that the dark is increased for low and high gains. At low gains the sensor is sensitive up to 3.5 um, therefore more sensitive to photon leakage, whereas at high gains the dark current is limited by trap assisted tunneling (TAT) effect.

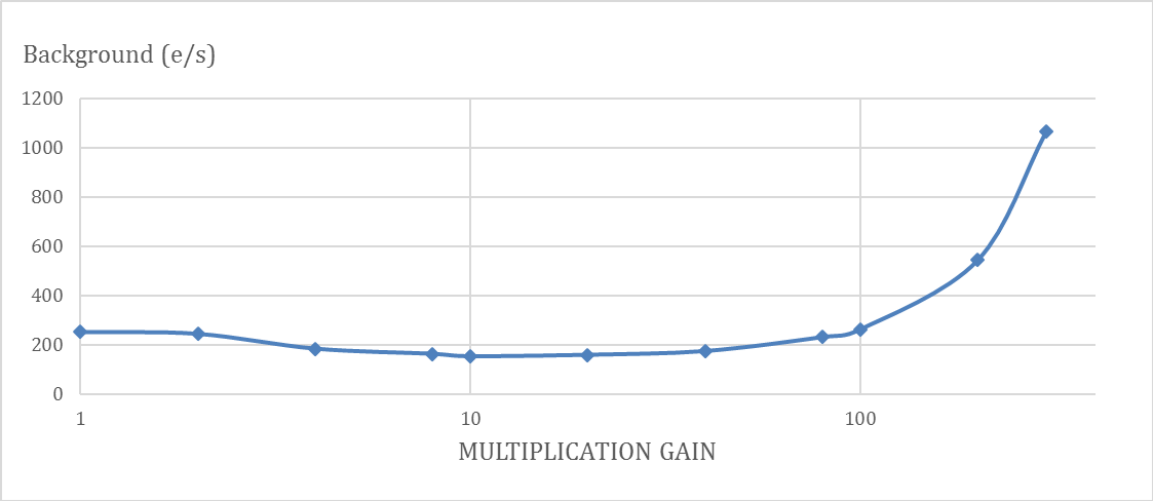

Fig. 11: C-RED One background when looking at a room temperature blackbody with F/4 beam aperture.

Cosmetics

One of the advantage of this sensor is its extremely good cosmetics, even when high gain is applied. Some other groups reported only a few dead pixels over the entire array, which is due to the HgCdTe growing process (MOVPE). Even with our engineering grade device, the cosmetics was excellent only showing a few pixels with leakage dark current (see Fig. 12). Shows images at various gains. e-APDs are not sensitive to degradation by image over-illumination.

Fig. 12: Low light scene imaged with gains of 1,6,13,45 and 90 (from left to right) showing only a few defective pixels at high gain (<10 defective pixels) on our engineering grade device, CDS readout at 1700 FPS.

Cropping

C-Red allows multiple region of interest readout (MROI).The sensor uses 32 output amplifiers in parallel therefore is virtually split in a square of 10 columns of 32 pixels and 256 rows. It is then possible to select one or more sub region by selecting any column and row number. Fig. 13 illustrates the MROI readout mode. The output geometry of the frame will always be rectangular. In this mode the maximal frame rate scales with the number of pixels read out, therefore extremely high frame rates may be used, even when using CDS or multiple readout.

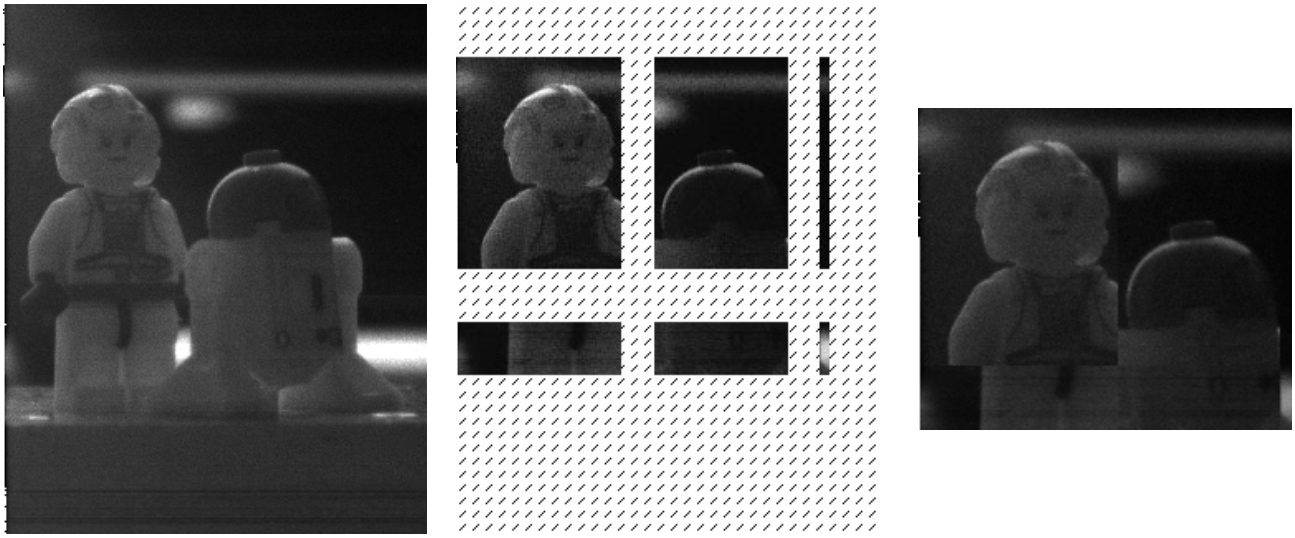

Full Frame ReadOut. 1700FPS *6 different regions. 3400FPS* *Raw Frame as sent by C-Red One.*

Fig. 13: Example of a cropping on Global Reset Mode with Correlated Double Sampling. The maximum frame rate increases with a reduction of the image size.

On-Board Bias Processing

C-RED One can compute by itself a bias image by meaning 1000 successive frames. This operation is done by the embedded software. Each frame outputs by the camera can then be subtracted by this bias image. It is also possible to send a custom bias to the camera or get the one computed on-board.

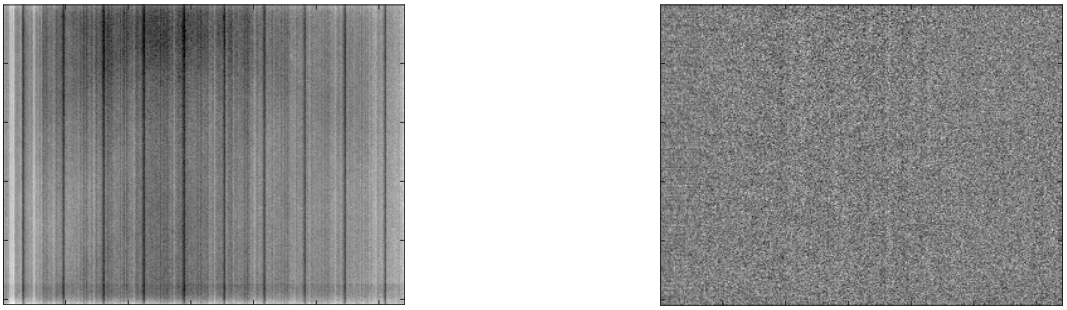

Fig. 14: Example of Bias Processing. Left: Raw Image. Right : Bias processed Image.

Multiple Non-Destructive Reads.

C-RED One can operate the sensor in multiple non-destructives reads mode. This mode permits to reset the focal plane once and then read a burst of frames.

Fig. 15 Bursts of multiple non-destructive reads.

The level will increase as electrons are accumulating in the integration capacitance. The slope will then provide information of flux.

This read out scheme allows reaching very low read out noise. It is used to compute the background in an original way.

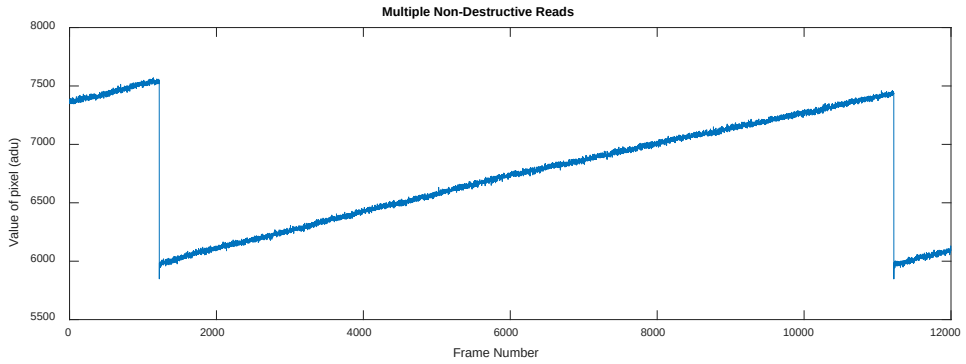

Fig. 16: 10 000 successive reads in Global Shutter mode. Hot subject seen through K and H filters at gain 1.

Bias Drift.

The mean level of some pixels is plot during 33 hours with a tick of 1s. C-RED One runs in Global Shutter mode with correlated double sampling at full speed.

Every mean level is processed with 100 samples to reduce the noise.

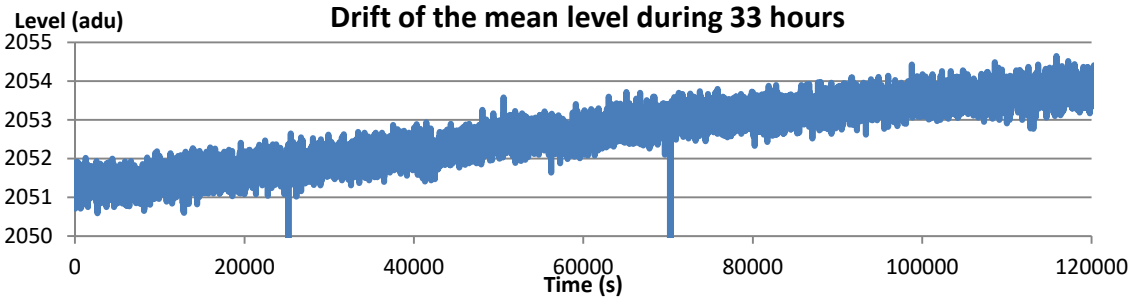

Fig. 17: Bias drift measurement over 33 hours.

Finally, the drift of C-RED One is as low as 0.1adu/h

3. THE C-RED 2 640X512 InGaAs SWIR camera from First Light Imaging

C-RED 2 is a revolutionary ultra high speed low noise camera designed for high resolution Short Wave InfraRed imaging based on the SNAKE detector from Sofradir [5], [6], [7], [8]. Thanks to its state of the art electronics, software, and innovative mechanics, C-RED 2 is capable of unprecedented performances: up to 400 images per second with a read out noise below 30 electrons. To achieve these breakthrough performances, C-RED 2 integrates a 640 x 512 InGaAs PIN Photodiode detector with 15 µm pixel pitch for high resolution, which embeds an electronic shutter with integration pulses shorter than 1 µs. C-RED 2 is also capable of windowing and multiple regions of interest (ROI), allowing faster image rate while maintaining a very low noise.

The software allows real time applications, and the interface is CameraLink full and superspeed USB3. C-RED 2 is designed to be updated remotely, and needs no human assistance to manage the cooling. The camera can operate in very low-light conditions as well as remote locations. Designed for high-end SWIR applications, smart and compact, C-RED 2 is operating from 0.9 to 1.7 µm with a very good Quantum Efficiency over 70%, offering new opportunities for industrial or scientific applications.

The Fig. 18 shows a picture of the C-RED 2 camera from First Light Imaging.

Fig. 18: the C-RED 2 InGaAs 640x512 SWIR camera from First Light Imaging offers unprecedented performances for this type of camera.

The Table 1 summarizes the main features and preliminary performances of the CRED-2 camera.

C-RED 2 PERFORMANCES

Test measurement	Result	Unit
Maximum speed	400	FPS
Mean Dark + Readout Noise at 400 fps	30	e-
Quantization	14	bit
Detector Operating Temperature	-40	C°
Flat Quantum Efficiency from 0.9 to 1.7 µm	>70	%
Operability	99.7	%
Image Full well capacity at low gain, 400 fps	1400	ke-
Image Full well capacity at high gain, 400 fps	43	ke-

MAIN FEATURES

- 640X512 InGaAs sensor
- 0.9 µm to 1.7 µm (70% QE)
- 15 µm pixel pitch
- Windowing and ROI
- Cooled sensor operation for low dark
- CameraLink or USB3 interface
- Optical interface: C-Mount
- 400 FPS Full Frame / 30 e^- Read Out Noise
- 10 e^- Read Out Noise / 25 FPS Full Frame
- < 1µs electronic shutter
- Cooling: Air or Liquid (Ambiant)
- Size: L 140 mm x W 75 mm x H 55 mm
- Weight: 0.9 kg

Table 1: typical performances and main features of the CRED-2 640x512 InGaAs SWIR camera.

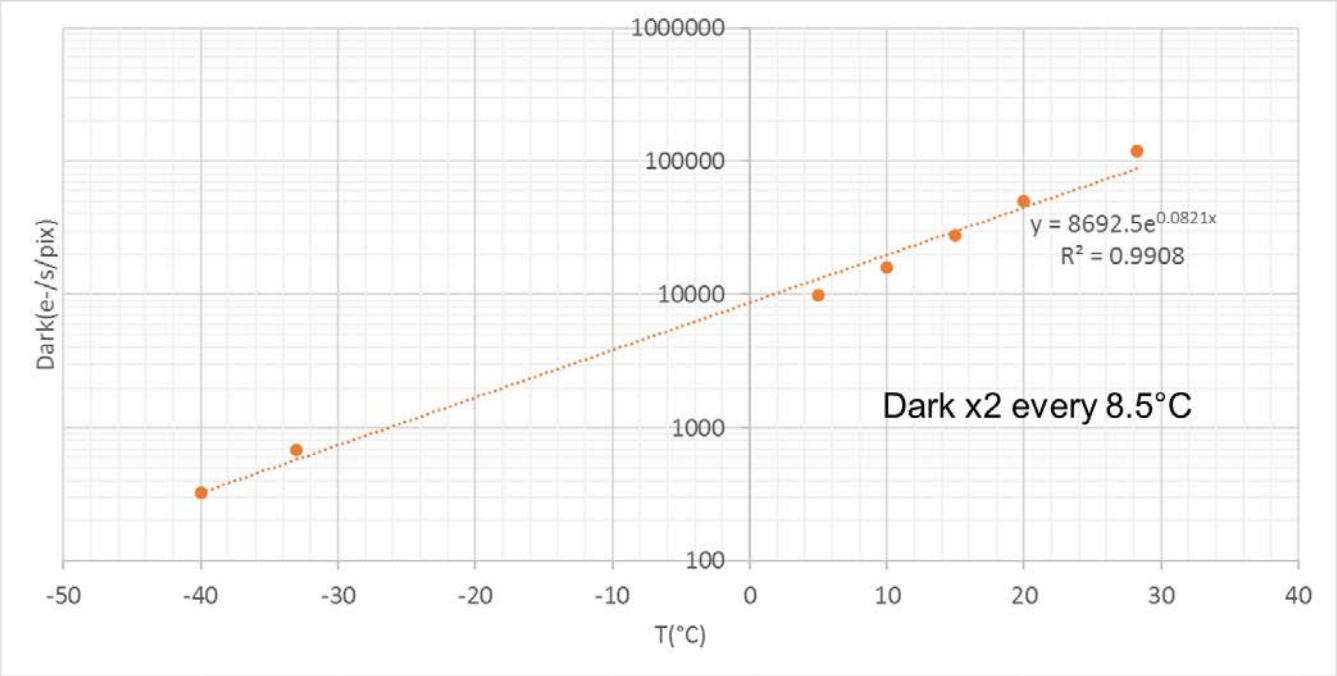

Fig. 19: C-RED 2 Dark (in e/s/pixel) as a function of the temperature (in °C).

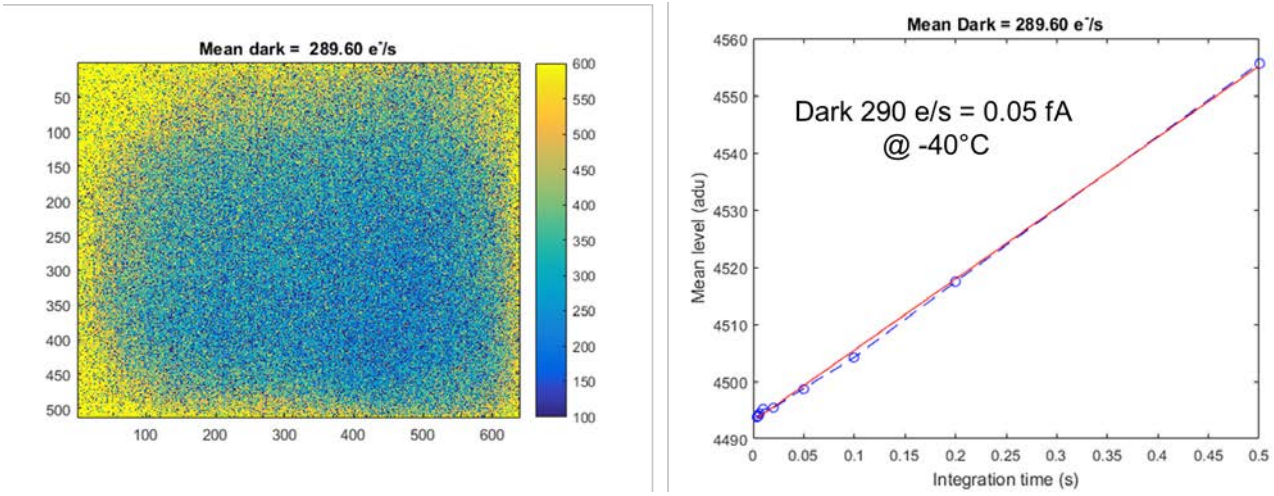

Fig. 20: (left) C-RED 2 dark image at -40°C, scale is in e/s; (right) Dark measurement at -40°C by measuring level as a function of the integration time. The camera system gain in 2.33 e/adu. Dark as low as 290 e/s (0.05 fA) is measured here at -40°C.

The Fig. 19 and Fig. 20 are showing the dark current measurement from C-RED2. It shows that the mean dark current is multiplied by a factor of 2 every 8.5 °C. It also shows that a mean dark current of 290 e/s (0.05 fA) is demonstrated at an operating temperature of -40°C. The value of 290 e/s is a simple average of the dark over all the pixels from the image without excluding the hot pixels from the statistics, demonstrating the highly mature detector technology of C-RED 2.

The Fig. 21 shows the readout noise of the C-RED 2 camera at 400 FPS in CDS mode (Correlated Double Sampling). A readout noise of 22 e is achieved at a readout speed of 400 FPS full frame. This type of performance in terms of speed and noise combined has never been achieved so far by the C-RED 2 competitors for a SWIR InGaAs VGA camera.

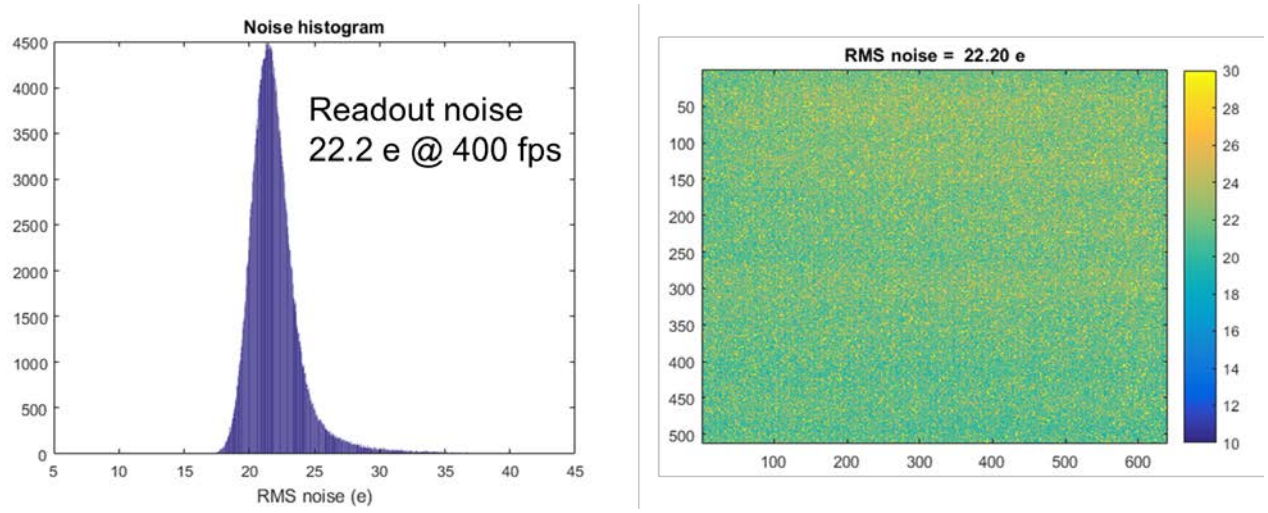

Fig. 21: (left) C-RED2 camera readout noise histogram at 400 frames/s and -40°C. The mean readout noise is 22.2 e; (right) readout noise image at at 400 frames/s and -40°C.

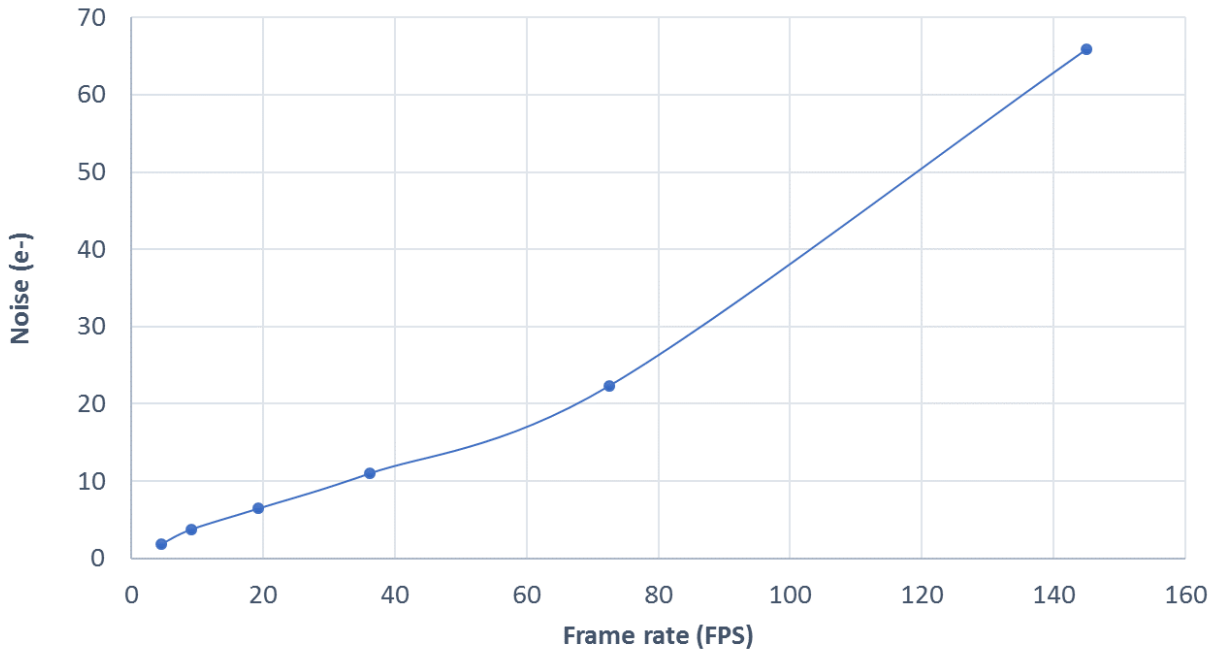

Fig. 22: C-RED 2 readout noise (in e) as a function of the frame rate (in FPS) in Non Destructive ReadOut (NDRO) mode.

The Fig. 22 shows the readout noise of the C-RED 2 camera in NDRO (Non Destructive ReadOut) mode. This special mode slows down the frame rate but at the same time allows to decrease the readout noise below 10 e at 25 FPS readout speed. Again, this has never been achieved on this type of SWIR cameras.

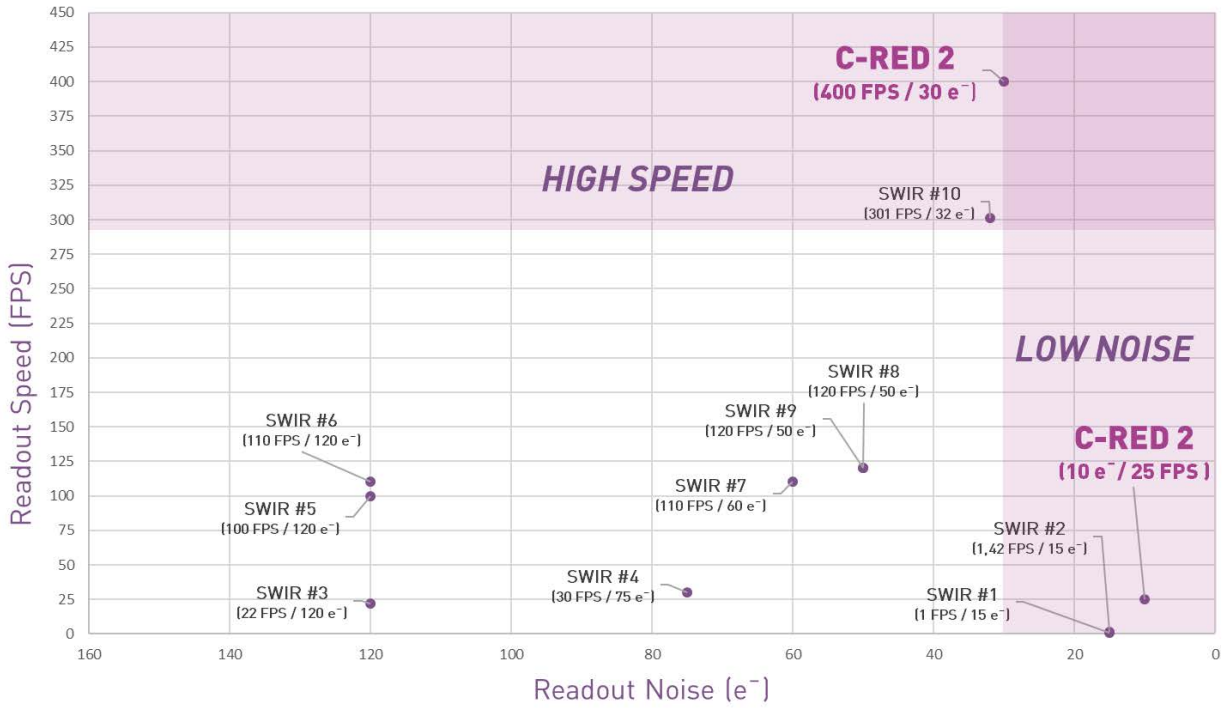

Fig. 23: the C-RED 2 camera compared to its SWIR main competitors.

The Fig. 23 compares the C-RED 2 camera in terms of noise and speed with its competitors, showing that C-RED 2 exceeds by far what is available so far on this market.

4. CONCLUSION

We've demonstrated the ability of CRED One to have comparable or even better performance than visible fast cameras dedicated to AO wavefront sensing like OCAM2 : this camera offers fast frame rate, subelectron noise, low background, wide spectral response over J, H and K bands, and outstanding cosmetics compared to other SWIR cameras. APD technology is now mature enough to be used in scientific applications. An unprecedented noise of 0.4 e was achieved for a SWIR camera at the incredible speed of 3500 FPS . C-RED one permits then a significant advance in short wave infrared imaging and is opening new windows for scientific applications like IR wavefront sensing or fast IR focal plane arrays used in astronomy.

In addition to the C-RED One development, C-RED 2 is InGaAs 640x512 fast camera with unprecedented performances in terms of noise, dark and readout speed based on the SNAKE SWIR detector from Sofradir. An incredible readout noise of 22 e has been obtained at 400 FPS readout speed in CDS mode. At 25 fps, the readout noise goes below 10 e. Cooled at -40°C, the C-RED 2 camera is able to achieve a dark current of 290 e/s (0.05 fA).

C-RED One and C-RED 2 are both SWIR commercial cameras from First Light Imaging fully available for ordering.

REFERENCES

[1] P. Feautrier et al., "OCam with CCD220, the Fastest and Most Sensitive Camera to Date for AO Wavefront Sensing", Publ. Astron. Soc. Pac. Vol 123 n°901, 263-274 (2011)

[2] J.L. Gach and P. Feautrier, “Electron initiated APDs improve high-speed SWIR imaging”, Laser Focus World vol 51 n°9, 37-39, (2015)
[3] G. finger et al., “Evaluation and optimization of NIR HgCdTe avalanche photodiode arrays for adaptive optics and interferometry”, Proc. SPIE 8453, 84530T (2012).
[4] Feautrier, Philippe, Gach, Jean-Luc, Wizinowich, Peter, "State of the art IR cameras for wavefront sensing using e-APD MCT arrays", AO4ELT4 Conference, 2015. Rouvié, O. Huet, S. Hamard, JP. Truffer, M. Pozzi, J. Decobert, E. Costard, M. Zécri, P. Maillart, Y. Reibel, A. Pécheur “SWIR InGaAs focal plane arrays in France”, SPIE Defense, Security and Sensing, 8704-2 (2013)
[5] Rouvié, O. Huet, S. Hamard, JP. Truffer, M. Pozzi, J. Decobert, E. Costard, M. Zécri, P. Maillart, Y. Reibel, A. Pécheur “SWIR InGaAs focal plane arrays in France”, SPIE Defense, Security and Sensing, 8704-2 (2013)
[6] J. Coussement, A. Rouvié, EH. Oubensaid, O. Huet, S. Hamard, JP. Truffer, M. Pozzi, P. Maillart, Y. Reibel, E. Costard, D. Billon-Lanfrey “New Developments on InGaAs Focal Plane Array”, SPIE Defense, Security and Sensing, 9070-5 (2014)
[7] Rouvié, J. Coussement, O. Huet, JP. Truffer, M. Pozzi, E.H. Oubensaid, S. Hamard, P. Maillart, E. Costard, “InGaAs Focal Plane Array developments and perspectives”, SPIE Electro-Optical and Infrared Systems, 9249 (2014)
[8] Rouvié, J. Coussement, O. Huet, JP. Truffer, M. Pozzi, E.H. Oubensaid, S. Hamard, V. Chaffraix, E. Costard “InGaAs Focal Plane Array developments and perspectives”, SPIE Defense, Security and Sensing, 9451-4 (2015)